J Korean Radiol Soc 2007;56:443 - 450

Noninvasive Assessment of In-Stent Restenosis of the Coronary Artery with Using 16-Slice Computed Tomography[1]

Eunhye Yoo, M.D., Byoung Wook Choi, M.D., Namsik Chung, M.D.[2], Jae Seung Seo, M.D., Young-Jin Kim, M.D., Tae Hoon Kim, M.D.[3], Kyu Ok Choe, M.D.

Purpose: We strove to evaluate in-stent restenosis of the coronary artery by measuring the in-stent CT attenuation with using 16-multislice CT.

Materials and Methods: We analyzed the coronary CT angiography, with using 16-slice CT, in 45 stents of 30 patients. The CT attenuation was measured in the lumen of the stented segments and in the lumen of the segment proximal to the stents, and this attenuation was compared with each other. The CT attenuation difference between them was analyzed in relation to the presence of significant in-stent restenosis. Conventional coronary angiography was used as a standard of reference for in-stent restenosis.

Results: 12 stents in 12 patients revealed significant restenosis on the conventional coronary angiography. In 6 (50%) of them, the CT attenuation value of the in-stent lumen was lower than that of the proximal segments (373.8 HU vs. 497.1 HU, respectively, $p=0.77$). In the other 6 stents, a small stent diameter ($n=3$) and adjacent severe calcification ($n=2$) accounted for the higher CT attenuation value of the in-stent lumen. In all the stents without significant restenosis, the CT attenuation values of the in-stent lumens were higher than those of their proximal segments.

Conclusion: The measurement of CT attenuation with using 16-slice CT at the in-stent lumen as compared to the attenuation of the proximal segment provides an objective, confident method for the diagnosis of in-stent restenosis.

Index words : Computed tomography (CT), helical
Coronary vessels, stents and prostheses

Percutaneous coronary angioplasty with stent insertion has been widely used for managing coronary artery occlusive disease. However, the risk of in-stent restenosis is about 10 - 40%, as determined on the angiographic follow-up at 6 months, and this remains a clinical issue in cardiology (1 - 3). Early identification of in-stent restenosis is important to reduce the number of recurrent ischemic episodes and to prevent myocardial infarction, thereby improving the long-term prognosis. Although routine follow-up angiography at 6 months is the most sensitive method to detect in-stent restenosis, non-invasive assessment of in-stent restenosis by multislice spiral computed tomography (MSCT) has the advantages of comfort, safety, time and cost when compared to conventional coronary angiography.

For the initial reports of in-stent visualization with us-

[1]Department of Diagnostic Radiology and the Research Institute of Radiological Science, Yonsei University College of Medicine, Severance Hospital, Seoul, Korea
[2]Department of Cardiology, Yonsei University College of Medicine, Seoul, Korea
[3]Department of Diagnostic Radiology, Yonsei University College of Medicine, Yong-Dong Severance hospital, Seoul, Korea
Received October 13, 2006 ; Accepted March 20, 2007
Address reprint requests to : Byoung Wook Choi, M.D., Department of Diagnostic Radiology, Yonsei University College of Medicine, 134 Sinchon-dong, Seodaemoon-gu, Seoul 120-752, Korea.
Tel. 82-2-2228-7400 Fax. 82-2-393-3035
E-mail: bchoi@yumc.yonsei.ac.kr

ing 4-detector CT, the most serious problems were partial volume effects and beam-hardening artifacts from the stents and motion artifacts from the pumping heart (4, 5). Several studies have recently reported improved visualization of in-stent stenosis by using 16-slice CT (6-11). However, even with using 16-slice CT, clear delineation of in-stent restenosis on visual assessment was not consistently possible. Therefore, we assessed the feasibility of evaluating in-stent restenosis with using 16-slice CT by measuring the CT attenuation of the in-stent lumen and comparing it to that of the proximal segments.

Materials and Methods

Subjects

We enrolled 32 consecutive patients who underwent both coronary CT angiography (CTA) and conventional angiography for determining the patency of a coronary artery stent. The patients were randomly referred for coronary CTA before undergoing conventional coronary angiography for following up the stent patency ($n=13$), or for evaluating chest pain ($n=13$), chest discomfort ($n=3$) or an abnormal treadmill test report ($n=2$). The institutional ethics committee approved the study and all the patients gave us their written informed consent. 32 coronary CT angiograms were reviewed for analysis of 48 stents. These stents included 13 Express (Boston Scientific, strut thickness=0.13 mm), 8 Arthos (AMG, 0.105 mm), 6 Nir (Boston Scientific, 0.102 - 0.109 mm), 2 Cypher (Cordis, 0.14 mm), 2 Jostent (Jomed, 0.09 mm), 1 Multilink Rx (Guidant, 0.9 - 0.1 mm), 1 GFX (AVE, 0.13 mm), 1 Biodiv Ysio (Biocompatibles, 0.06 mm), 1 Bx sonic (Cordis, 0.14 mm), 1 Coroflex (B. Braun, 0.1 mm), 1 Crossflex (Cordis, 0.14 mm), 1 Microstent (AVE, 0.1 mm), 1 Radius (Boston Scientific, 0.102 - 0.109 mm) and 9 unknown stents. All the known stents, except one, were made of stainless steel. Sixteen stents were bare metal stents and the other 23 stents were drug-eluting stents.

Three stents (6%) in 3 patients were excluded from analysis because the quality of the coronary CTA was not good enough to be reviewed. The poor quality of these particular CTAs was due to severe motion artifacts, one of which occurred from respiratory motion and the others occurred due to cardiac arrhythmia during scanning. 45 stents (1.5 stents/patient) in 30 patients (25 men, age range: 59±12 years) were included for analysis. These stents were located at the left anterior descending artery (LAD: $n=21$, proximal: 8, mid: 9, distal: 4), the left circumflex artery (LCx: $n=11$, proximal: 4, mid: 3, distal: 4), the right coronary artery (RCA: $n=12$, proximal: 7, mid: 3, distal: 2), and the saphenous venous graft (SVG: $n=1$) from the ascending aorta to the right coronary artery. The time interval between the coronary arterial stenting and the coronary CTA was 2 ±2.4 years (range: 1 day to 8 years). The stent diameters from 35 of the 45 stents were measured (3.1±0.5 mm, range: 1.6 - 4.0 mm).

Coronary CT Angiography

Coronary CTA was performed with using a 16-slice MSCT scanner (Sensation 16, Siemens, Forchheim, Germany). Those patients with a heart rate more than 65 beats per minute were pre-treated one hour prior to the CT scan with 30 - 50 mg of propranolol in order to lower their heart rate. During scanning, the mean heart rate of all the patients was 60±8.8 beats/min (range: 57 to 91 beats/min). 100 to 120 mL of nonionic contrast agent (370 iodine mg/mL, Iopamiro; Bracco, Milano, Italy) was injected via an 18 - or 20 - gauge needle through an antecubital vein with using a flow rate of 4 mL/s. A real-time bolus tracking technique was used for triggering the scan. We obtained a volume data set from the carina to the diaphragm during a single inspiratory breath-hold (duration: 19.2±2.2 s). The CT parameters were a gantry rotation time: 0.42s, table-feed: 3.4 mm/rotation, collimation: 16×0.75 mm, tube current: 500 effective mA at 120 kV, field of view: 220 mm and matrix: 512×512. By performing retrospective ECG-gated reconstruction, the transaxial images were created with a slice thickness of 1.0 mm and an increment of 0.5 mm at the minimal motion point through the cardiac cycle. A medium-smooth kernel (B30f) was used for the angiographic images. Multi-cyclic segmented reconstruction was applied and the temporal resolution ranged from 110 to 210 ms.

MSCT Data Analysis

For the CTAs, the multi-planar images were reformatted with a slice thickness of 1 mm and an increment of 1 mm in order to show the cross-sectional views of individual stents. The CT attenuation values of the in-stent lumens were measured by establishing regions of interest (ROIs). Two experienced radiologists, who worked in consensus, drew the ROI on every cross sectional view of each stent (Fig. 1). The ROI was consistently drawn along the inner border of the stent wall under a

setting of 5,000 Hounsfield Units (HU) for the window width and a level of 200 HU to improve the delineation of the real stent size (12). We also measured the CT attenuation values on the cross-sectional view of the segments that were proximal to the stents; these segments had the largest area within a 2 cm distance from the stents and they were not combined with the stenosis, if possible. If there were greater than or equal to 3 consecutive slices in the in-stent lumen that had a lower attenuation value than its proximal segment, then significant in-stent restenosis was considered to be present. In these cases, the CT attenuation value of the slice that had the lowest value of those consecutive slices was used as the CT attenuation value of its in-stent lumen. For the other cases in which the CT attenuation value of the in-stent lumen was equal to or greater than that of its proximal segment, the average CT attenuation value of the center slice of 3 evenly divided segments along the longitudinal axis of the stent was used as the CT attenuation value of its in-stent lumen.

Conventional X-ray Coronary Angiography

Conventional X-ray coronary angiography was performed using a time interval of 8.5±9.3 days (range: 1 to 35 days) after the CTA. Coronary angiography was performed using the Judkins technique and this was recorded at 30 frames/sec in multiple projections. Significant restenosis was defined when the narrowing of the lumen diameter was equal to or greater than 50% and this included total occlusion (100% narrowing). Two cardiologists working in consensus assessed the coronary angiograms.

Statistical Analysis

Two-sample t-tests and paired t-tests were used for statistical analysis. A p-value of < 0.05 was considered to be statistically significant.

Results

Twelve stents in 12 patients (12/45, 27%) revealed significant restenosis according to conventional x-ray coronary angiography. Among these 12 stents, 4 showed total occlusion and eight showed narrowing equal to or greater than 50% and less than 100% of the diameter determined on the conventional coronary angiography. The mean diameter of the stents that had significant restenosis ($n=11$) was 2.9±0.6 mm with a range of 1.6-3.5 mm, which was not significantly different from that of the stents without significant restenosis ($n=24$, mean diameter: 3.1±0.4 mm, range: 2.7 - 4.0 mm). The time interval between stent insertion and the coronary CTA for the significant restenosis group was 3.4±2.9 years, which was significantly longer than that of the stents without significant restenosis (1.3±1.9 years). Those stents with significant restenosis were in the LAD ($n=5$ stents, proximal LAD: 2, middle LAD: 2, distal LAD: 1), in the LCx ($n=3$ stents, proximal LCx: 1, middle LCx: 2), and in the RCA ($n=$ 4 stents, proximal RCA: 3, middle RCA 1).

The CT attenuation value of the in-stent lumens without significant restenosis was significantly greater than

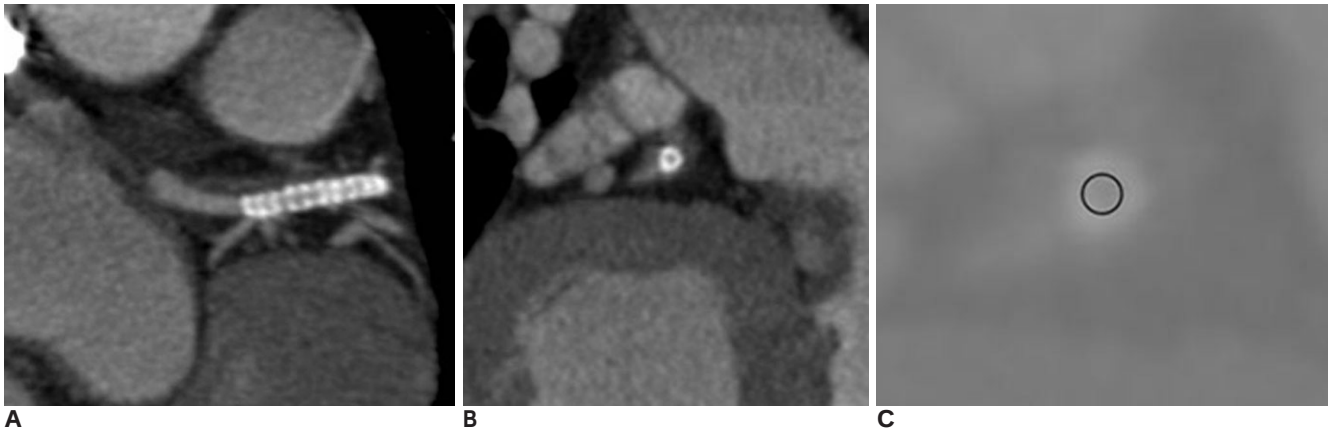

A **B** **C**

Fig. 1. Measurement of the in-stent lumen CT attenuation values of the longitudinal (**A**) and cross sectional view (**B**) multiplanar reformatted (MPR) images of the proximal left anterior descending (LAD) artery shows an in-stent lumen obscured by the stent struts. The CT attenuation values of the in-stent lumen are measured by the ROI on each of the cross sectional views under a setting of a window width of 5000 HU and a level of 200 HU (**C**), and then these are compared with the CT attenuation value of its vascular segment proximal to the stent.

that of their proximal segments (429±57 HU vs. 330±44 HU, respectively, $p=0.001$) (Fig. 2). This higher attenuation of the in-stent lumen compared with that of the normal segments was partly due to the high density of the blooming artifact from the stents. However, the CT attenuation value of the in-stent lumens with significant restenosis was not significantly different from that of their proximal segments (335±149 HU vs. 333±84 HU, respectively $p=0.96$). The difference of CT attenuation between the lumens of the in-stent and proximal segments (= the CT attenuation of the in-stent lumen - the CT attenuation of their proximal segment) in the stents without significant restenosis was significantly greater than those with significant restenosis (100±56 HU vs. 1.6±106 HU, respectively $p=0.008$) (Table 1). In all the stents without significant restenosis, the CT attenuation values of the in-stent lumens were always higher than those of their proximal segments. In contrast, for six (50%) of the 12 stents with significant restenosis, the CT attenuation value of the in-stent lumen was lower than that of the proximal segment (373.8 ±90 HU vs. 497.1±59.5 HU, respectively, $p=0.77$) (Fig. 3). The minimal CT attenuation pixel values in these six stents ranged from 20 to 110 HU, and they were significantly lower than the values of the stents without significant restenosis (77±35 HU vs. 353±68 HU, respectively, $p=0.001$, range of CT attenuation values of stents without significant restenosis: 227 - 502 HU). Three of these 6 stents were totally occluded (75% of the totally occluded stents) and 3 were narrowed (38% of the stents with 50% ≤ narrowing < 100%).

The difference of CT attenuation values between the lumen of the stented segments and the segments proximal to the stents for the other six of the 12 stents with significant restenosis (false negative) was not significantly different from the difference of that for the stents without significant restenosis (93±58 HU vs. 100±56 HU, respectively, $p=0.7$). Three of the false negative cases (50%) had lumens less than 3 mm in diameter, with the narrowest stent diameters being 1.6, 2.2 and

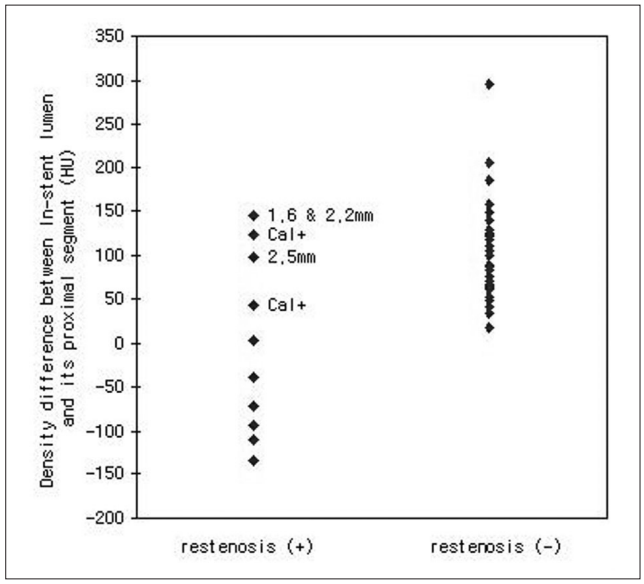

Fig. 3. CT attenuation differences between the in-stent lumen and its proximal segment in the stents with and without significant restenosis.
The false negative cases were labeled with their causes of higher-than-expected in-stent luminal CT attenuation values, including the small stent diameter of 3 stents and the presence of severe calcification (Cal+) on 2 stents.

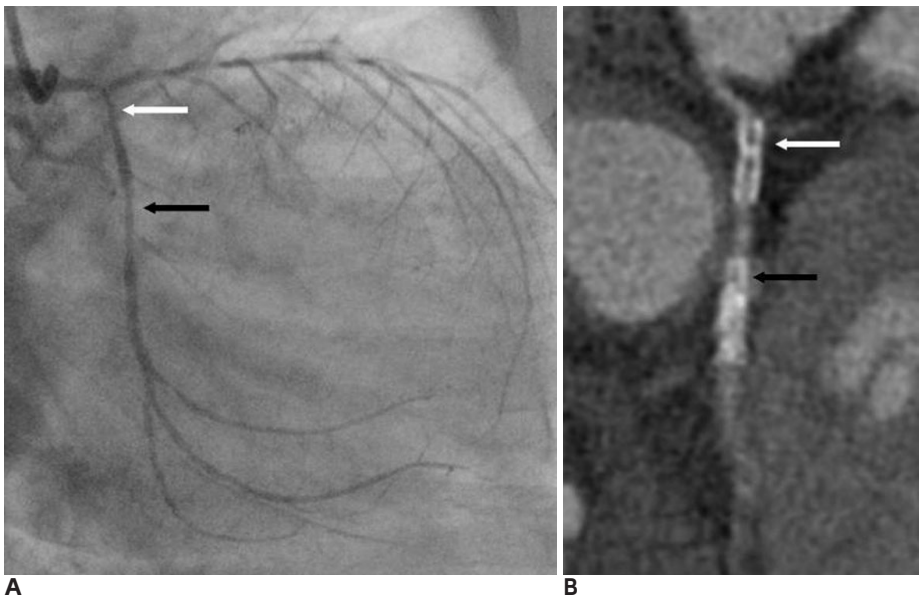

Fig. 2. 66-year-old man with in-stent restenosis in the left circumflex artery (LCx).
The conventional coronary angiogram (**A**) displays in-stent restenosis of the proximal (white arrow) and middle (black arrow) LCx. Measurement of the in-stent lumen attenuation is lower than the proximal segment attenuation on the longitudinal MR image of the proximal LCx (**B**, white arrow), which is considered as in-stent restenosis. The stent lumen of the middle LCx (**B**, black arrow) is not visualized on CT, so it is impossible to evaluate the stent patency. (This stent was excluded from the study.)

2.5 mm, respectively. Two of the false negative cases (40%) had severe calcification around the stents. The other false negative case showed very similar CT attenuation values between the in-stent lumen and the proximal segment with the difference being only 3.6 HU. The strut thickness of these 6 stents was not different from those of the other 6 stents with restenosis or those of the other stents without restenosis.

Five stents had mild restenosis that was less than 50% of the diameter (range: 10 - 45%). These stents had a slightly lower difference between the CT attenuation values of the in-stent lumens and their proximal segments compared to that of the stents without any stenosis (59±.41 HU Vs. 108±55 HU, respectively, $p=0.04$). All the segments distal to the stents showed the filling-in of contrast agent except for one of the 4 occluded stents.

When we included only the 28 stents that greater to or equal to 3.0 mm in length among the 35 stents with a known stent size, significant restenosis greater or equal to 50% was observed in 8 stents (with total occlusion in 4), mild stenosis less than 50% was observed in 4 stents, and no stenosis was observed in 16 stents. Table 1 summarizes the frequency of stenosis, according to the range of CT attenuation value differences, which were defined by using the mean difference of the values of each group for the stents greater than 3.0 mm in size.

Discussion

MSCT can evaluate, with limited accuracy, in-stent

Table 1. CT Attenuation Differences Between the in-stent Lumen and the Proximal Segments

	All Stents ($n=45$)	Stents ≥ 3.0 mm ($n=28$)
Without Any Stenosis	108±55 HU ($n=28$)	98±43 HU ($n=16$)
0% < Mild Stenosis ≤ 50%	59±41 HU ($n=5$)	45±30 HU ($n=4$)
50% < Significant Stenosis ≤ 100%	1.6±106 HU ($n=12$)	- 52±83 HU ($n=8$)
Total Occlusion = 100%	- 48±118 HU ($n=4$)	- 48±118 HU ($n=4$)

Table 2. The Degree of Stenosis seen on Conventional Coronary Angiography versus the CT Attenuation Difference between the In-stent Lumen and the Proximal Segment for Stents Greater or Equal to 3.0 mm ($n=28$)

Attenuation Difference (D)	Without Any Stenosis	Mild Stenosis	Significant Stenosis
D > 98 HU	8	0	1*
98 ≥ D > 45 HU	8	1	0
45 ≥ D > - 52 HU	0	3	2†
- 52 > D	0	0	5‡

The numbers are frequencies.
* Occluded stent case with severe calcification
† No occluded stents
‡ Including 3 occluded stents
Mild stenosis means the diameter narrowing was equal to or greater than 50%
Significant stenosis means the diameter narrowing was lesser than 50%

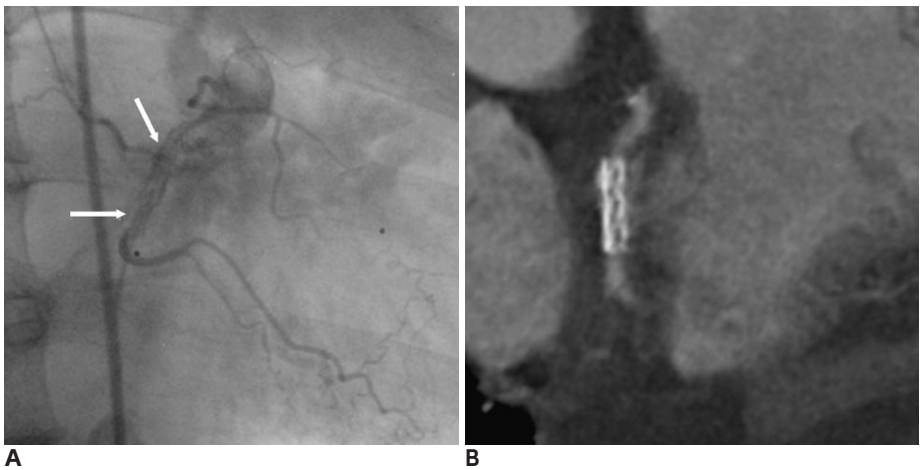

Fig. 4. 50-year-old man with in-stent occlusion with collateral flow to the distal segment
The conventional coronary angiogram (**A**) displays in-stent occlusion of the proximal right coronary artery (RCA, arrows) with a TIMI grade 1 collateral. Longitudinal MPR image (**B**) of the proximal RCA shows a lower-attenuation area within the in-stent lumen than that in the vessel proximal to the segment, but an enhanced distal vascular segment is seen.

restenosis of the coronary artery. Many factors affect this accuracy, and these factors can be classified into four categories; 1) stent factors, 2) calcification at the stent site, 3) imaging factors, and 4) the standard or criteria for the decision.

An early study with 4-detector CT reported that in-stent lumens could not be visualized, and this was mainly due to partial volume effects and beam hardening artifacts of the metallic stent material (4). However, with using 16-slice MSCT, evaluation of in-stent restenosis was feasible even though many cases should have been excluded from analysis (33%) (13). The reasons for exclusions are a small stent size and metal artifacts. In a previous study using 16-slice MSCT, those stents less than or equal to 3.0-mm were almost impossible to evaluate (6). In our study, significant restenoses in the stents with a diameter less than 3.0-mm were misdiagnosed. The severity of artifacts from stents is also related to the stent material. Gilard et al. (6) reported that 93% of stainless steel stents were analyzable without any serious partial volume effect or beam hardening. Calcification was another important factor that induced beam hardening artifacts and partial volume effects (6, 10). In our present study, two of the false negative cases (40%) had severe calcification around the stents.

In general, imaging factors affect the overall image quality. The most important and frequent problem in coronary artery imaging has been motion artifacts. Evaluation of in-stent restenosis with MSCT was not feastable for those patients with arrhythmia and high heart rates (6, 8). However, motion artifacts can be controlled by reducing the heart rate with β-blockers, and by employing multi-cyclic segmented reconstruction and an optimized reconstruction window for the cardiac phase with minimal motion.

In an earlier study that used 4-detector CT and in some recent studies that used 16-slice CT, perfusion of the vessel distal to the stent was considered to be evidence of stent patency (4, 9, 11, 13). However, in our study, well-opacified segments were found distal to the occluded stents, in which collaterals seemed to cause retrograde opacification of the entire vessel distal to the stent occlusion (Fig. 4). Therefore, the opacified vessel distal to the stent cannot be used as evidence for stent patency.

Evaluation of in-stent restenosis with CT has depended on visual assessment. In previous studies that had a wide range of exclusion from 1.3 to 31.1% and a prevalence of significant restenosis from 8.1 to 23.8%, the sensitivity and specificity ranged from 78 to 100% and from 92 to 100%, respectively (6, 8, 9, 11, 13). In one study, occlusion was determined to be present when the lumen inside the stent was darker than the contrast-enhanced vessel before the stent, and non-occlusive stent restenosis was determined to be present when the lumen inside the stent showed an eccentric or concentric darker rim (8). However, metallic artifacts from the stent strut might usually obscure the low density in the periphery of the lumen, which is where neointimal hyperplasia starts at. In a previous study, the presence of neointimal proliferation less than 35% could not be distinguished with using 16-slice MSCT because of its insufficient spatial resolution (6). Furthermore, according to our study, either occlusion or non-occlusive significant restenosis was present when the in-stent lumen had a lower CT attenuation than the contrast-enhanced vessel before the stent. Therefore, visual assessment may be subjective, inaccurate and irreproducible. The pixel counting method is the only objective method that has ever been reported to use CT attenuation measurements to diagnose-stent restenosis (10).

To date, the previous studies that have used MSCT have used the same principles, that is, neointimal hyperplasia had a lower CT attenuation than the contrast-enhanced vessel lumen. The lowest pixel values of the in-stent lumens, which were correctly diagnosed as significant restenosis in the present study, were similar to the CT values of neointimal hyperplasia in the carotid artery (77±35 HU vs. 75.6±5.6 HU, respectively) (14). Although low attenuation values were detected only in the significant stenosis cases, these low values can be evidence that some degree of neointimal hyperplasia is present in the stent. For the cases of mild narrowing less than 50%, the difference between the CT attenuation of the in-stent lumen and its proximal segment was significantly different from that of the stents without any degree of stenosis. However, the ranges of the differences considerably overlapped each other.

In summary, the present study showed that measuring in-stent luminal CT attenuation could not easily differentiate between significant in-stent restenosis and insignificant restenosis or no stenosis, even with exclusion of those cases with motion artifacts. The small stent size and severe calcification were presumed to be main causes of the erroneous measurement of the attenuation value in the stented lumen. In practice, small stents less than 3.0-mm and stents with severe calcification should be excluded from this type of analysis. If CTA is per-

formed in a well-controlled manner for selected cases, then the image quality would be good enough for visualizing the in-stent lumen and measuring the CT attenuation in the lumen.

Our study was limited only to stainless steal stents and we did not study the effect of stent design. Calcification could affect the measurements of CT attenuation at the segment proximal to the stent. Sharp-kernel images of CTA were not used in the present study, and these images have been reported to be useful to reduce the 'blooming artifact' of the metallic stent (15). Although a sharp-kernel was helpful for achieving more accurate measurement of the in-stent lumen diameter, the sharp-kernel usually increased the noise level, which was then not optimal for evaluating the unstented coronary artery segments (12). In the present study, an extremely large window width (5,000 HU) was used for better delineation and more accurate measurement of the in-stent lumen. Despite these limitations, the CT attenuation measurement provided an objective and confident diagnosis when evaluating significant in-stent restenosis via 16-slice MSCT. This method should be more accurate and complementary to visual assessment with using more advanced CTA technology, in which the in-stent luminal restenosis can be clearly visualized and quantified in a diameter or an area.

References

1. Antoniucci D, Valenti R, Santoro GM, Bolognese L, Trapani M, Cerisano G, Boddi V, Fazzini PF. Restenosis after coronary stenting in current clinical practice. *Am Heart J* 1998;135(3):510-518
2. Elezi S, Kastrati A, Hadamitzky M, Dirschinger J, Neumann FJ, Schomig A. Clinical and angiographic follow-up after balloon angioplasty with provisional stenting for coronary in-stent restenosis. *Catheter Cardiovasc Interv* 1999;48(2):151-156
3. Ruygrok PN, Webster MW, de Valk V, van Es GA, Ormiston JA, Morel MA, Serruys PW. Clinical and angiographic factors associated with asymptomatic restenosis after percutaneous coronary intervention. *Circulation* 2001;104(19):2289-2294
4. Kruger S, Mahnken AH, Sinha AM, Borghans A, Dedden K, Hoffmann R, Hanrath P. Multislice spiral computed tomography for the detection of coronary stent restenosis and patency. *Int J Cardiol* 2003;89(2-3):167-172
5. Maintz D, Grude M, Fallenberg EM, Heindel W, Fischbach R. Assessment of coronary arterial stents by multislice-CT angiography. *Acta Radiol* 2003;44(6):597-603
6. Gilard M, Cornily JC, Rioufol G, Finet G, Pennec PY, Mansourati J, Blanc JJ, Boschat J. Noninvasive assessment of left main coronary stent patency with 16-slice computed tomography. *Am J Cardiol* 2005;95(1):110-112
7. Maintz D, Seifarth H, Flohr T, Kramer S, Wichter T, Heindel W, Fischbach R. Improved coronary artery stent visualization and in-stent stenosis detection using 16-slice computed-tomography and dedicated image reconstruction technique. *Invest Radiol* 2003; 38(12):790-795
8. Cademartiri F, Mollet N, Lemos PA, Pugliese F, Baks T, McFadden EP, Krestin GP, de Feyter PJ. Usefulness of multislice computed tomographic coronary angiography to assess in-stent restenosis. *Am J Cardiol* 2005;96(6):799-802
9. Kitagawa T, Fujii T, Tomohiro Y, Maeda K, Kobayashi M, Kunita E, Sekiguchi Y. Noninvasive assessment of coronary stents in patients by 16-slice computed tomography. *Int J Cardiol* 2005;108: 188-194
10. Ohnuki K, Yoshida S, Ohta M, Mochizuki S, Nishioka M, Sakuma T, Fukuda K, Ishizaki M, Hirakawa E, Andou T. New diagnostic technique in multi-slice computed tomography for in-stent restenosis: pixel count method. *Int J Cardiol* 2006;109:251-258
11. Schuijf JD, Bax JJ, Salm LP, Jukema JW, Lamb HJ, van der Wall EE, de Roos A. Noninvasive coronary imaging and assessment of left ventricular function using 16-slice computed tomography. *Am J Cardiol* 2005;95(5):571-574
12. Hong C, Chrysant GS, Woodard PK, Bae KT. Coronary artery stent patency assessed with in-stent contrast enhancement measured at multi-detector row CT angiography: initial experience. *Radiology* 2004;233(1):286-291
13. Schuijf JD, Bax JJ, Jukema JW, Lamb HJ, Warda HM, Vliegen HW, de Roos A, van der Wall EE. Feasibility of assessment of coronary stent patency using 16-slice computed tomography. *Am J Cardiol* 2004;94(4):427-430
14. Cademartiri F, Mollet N, Nieman K, Krestin GP, de Feyter PJ. Images in cardiovascular medicine. Neointimal hyperplasia in carotid stent detected with multislice computed tomography. *Circulation* 2003;108(21):e147
15. Maintz D, Juergens KU, Wichter T, Grude M, Heindel W, Fischbach R. Imaging of coronary artery stents using multislice computed tomography: in vitro evaluation. *Eur Radiol* 2003;13(4): 830-835

대한영상의학회지 2007;56:443 - 450

16-Slice CT를 이용한 관상 동맥 Stent 재협착의 비침습적 평가[1]

유은혜 · 최병욱 · 정남식[2] · 서재승 · 김영진 · 김태훈[3] · 최규옥

[1]연세대학교 세브란스병원 영상의학과
[2]연세대학교 세브란스병원 심장내과
[3]영동세브란스병원 영상의학과

목적: 16-절편 CT 관동맥조영술에서의 관동맥 스텐트 내강의 감쇠치(attenuation value)를 이용하여 스텐트 재협착을 비침습적으로 평가하고자 하였다.

대상과 방법: 16-slice CT로 coronary CT angiography 시행한 30명 환자의 stents 45개를 분석하였다. Stent 내강과 근위부 정상 관상동맥 분절에서 CT 감쇠치를 서로 비교하여 그 감쇠치차와 stent 재협착 정도간의 연관성을 파악하였다. 이때 고식적 혈관 촬영술을 기준으로 삼고 비교하였다.

결과: 고식적 혈관 촬영술에서 12명 환자의 12개 stents에서 유의한 재협착을 보였고 이들 중 6개에서 stent 내강의 CT 감쇠치가 근위부 동맥의 값보다 더 낮았다. 다른 6개 stents에서는 stent 내강의 감쇠치가 더 높았는데 이들 중 3개 stents는 직경이 작았고, 2개는 석회가 동반되었다. 유의한 재협착이 없었던 stents 모두에서 stent 내강 감쇠치는 근위부 동맥에서보다 더 높았다.

결론: stent 재협착 진단에 있어 16-slice CT에서의 stent 내강과 근위부 관상 동맥의 감쇠치 비교는 객관적인 방법이다. 작은 직경의 stent나 심한 석회화는 이 방법에서 부정확한 결과를 일으키는 주요 원인이다.